Supplement of

Landscape position and source, more than reactive metals, shape the molecular composition of organic matter in a volcanic-influenced old-growth mangrove soil (Panay Island, Philippines)

Ayaka Nishikawa, Toshihiro Miyajima, Raghab Ray, Ryan Basina, Maria Lourdes San Diego-McGlone, Charissa Ferrera, Morimaru Kida

Correspondence: Morimaru Kida (email)

Contents

S1 Acid pre-treatment test
S2 Procedural blanks and filtration
S3 Extraction temperature for pyrophosphate-extractable Fe and Al
Table S1 Sensitivity of exchangeable Ca and Mg to the pore-water correction
Table S2 Sensitivity of the whole-composition analyses to spectral binning
Figure S1 ^{1}H NMR spectra of triplicate extractions
Figure S2 ^{1}H NMR spectra of the four cores at 30–35 cm
Figure S3 Variation partitioning of NMR composition

S1 Acid pre-treatment test

Acid pre-treatment breaks bonds between organic matter (OM) and polyvalent cations and is commonly used to raise alkali extraction yields (Japanese Humic Substances Society, 2007). We tested it before the main analyses. Fine earth (0.1 g) was left overnight with 1 mL of 2 M HCl, centrifuged (15,000 rpm, 5 min), washed three times with ultrapure water and dried at 60 °C; untreated subsamples served as controls. Both were extracted with 0.1 M NaOH (1:10) for extracted OC (n = 8) and with 0.1 M NaOD at a carbon-to-solution ratio of 1:300 for ^{1}H NMR (n = 5). After NMR, 0.3 mL of each extract was diluted 50-fold in 0.05 M $Na_4P_2O_7$ (to keep Fe, Mn and OC in solution) and Fe and Mn were determined by ICP-OES with Y as internal standard.

Pre-treatment did not significantly increase OC extraction yields (paired two-sided t-test, n = 8, t = −2.19, p = 0.065). It raised Fe in the NMR extracts from 8.8–24.5 to 17.5–312 mg L^{-1} and Mn from 0.07–0.16 to 0.08–0.80 mg L^{-1}, lowering the molar OC:Fe ratio from 108–382 to 14–191. Spectra of most pre-treated extracts showed no usable signal, also when acquired with a single pulse or solvent presaturation instead of WATERGATE (one sample tested), consistent with paramagnetic relaxation by Fe and Mn. Acid pre-treatment was therefore omitted.

S2 Procedural blanks and filtration

Procedural blanks (0.1 M NaOD taken through the full extraction) contained < 2 % of sample OC but produced NMR signals that overlapped sample spectra. We compared four conditions: (a) solvent only, transferred directly to the NMR tube; (b) disposable syringe with rubber plunger and unrinsed glass-fiber syringe filter (Whatman Puradisc 13, 0.7 µm); (c) all-plastic syringe with unrinsed filter; and (d) all-plastic syringe with syringe and filter rinsed with 4 × 200 µL ultrapure water and 1 × 100 µL D_2O (triplicate blanks). Condition (b) gave sharp peaks at 2.4–2.7 ppm, and both (b) and (c) gave signals at 2.5–3.5 ppm; these were absent in (d), identifying the filter as their source. A weak signal near 1.3 ppm remained in all blanks, including the solvent blank, and is therefore common to all samples. Condition (d) was used for all samples.

S3 Extraction temperature for pyrophosphate-extractable Fe and Al

Pyrophosphate extractions performed in June and November gave systematically different results. To test whether laboratory temperature was responsible, test samples were extracted sequentially with pyrophosphate (16 h), acid oxalate (4 h, dark) and dithionite-citrate (16 h) (Wagai et al., 2018, 2020) at 5 and 25 °C, with centrifugation at c. 26,000 g for 45 min between steps. Extraction at 25 °C recovered 1–3 times more Fe and Al than at 5 °C in all fractions except dithionite-citrate Fe of one sample, with the largest difference in the pyrophosphate step. All pyrophosphate data reported in the main text were therefore obtained in June or at a controlled 25 °C.

Table S1

Table S1. Sensitivity of exchangeable Ca and Mg to the pore-water correction. Exchangeable cations were calculated as $X_{ex} = X_{measured} - f \times W \times C_{sw}$, where W is water per unit dry soil and C_{sw} is the seawater concentration; f scales pore-water salinity relative to seawater (f = 1 used in the main text; f = 1.09 corresponds to the pore-water vs creek-water salinity ratio at the site). ρ: Spearman correlation with OC content (n = 50). Partial R^2 and p: within-core association of Ca_{ex} with the five-region NMR composition (redundancy analysis of clr coordinates conditioned on core; 9999 permutations within cores), as in Table 2.

f	Samples with Mg_{ex} < 0	ρ(Ca_{ex}, OC)	ρ(Ca_{ex} + Mg_{ex}, OC)	Partial R^2 (Ca_{ex})	p
0	0	0.73	0.80	0.027	0.327
0.8	0	0.69	0.70	0.031	0.287
1	2	0.67	0.64	0.034	0.265
1.09	3	0.67	0.63	0.035	0.253
1.2	7	0.65	0.61	0.037	0.241

Table S2

Table S2. Sensitivity of the whole-composition analyses to spectral binning. The five literature regions (main text) are compared with 0.02 ppm bins over 0.5–4.3 and 5.3–8.4 ppm and with region-specific bins (0.04 ppm at 0.7–4.3 ppm, 0.2 ppm at 6.0–8.2 ppm). Zero cells (bins ≤ 0) were replaced by Bayesian-multiplicative replacement (Martín-Fernández et al., 2015) before clr transformation. Replicate/sample: mean Aitchison distance among K22-106 triplicate extractions divided by the median distance between samples. Core R^2: PERMANOVA. The five-region row here is computed from the processed spectra and may differ slightly from values based on the reported region proportions. Unique fractions: adjusted R^2 from variation partitioning (negative values ≈ 0).

Parts	n parts	Zero cells	Replicate/sample	Core R^2	Unique: metals	Unique: source
Five regions	5	0	0.35	0.42	0.062	0.105
0.02 ppm bins	345	234	0.67	0.10	0.031	0.028
0.04/0.2 ppm bins, trimmed windows	101	0	0.37	0.29	0.060	0.141

Figure S1

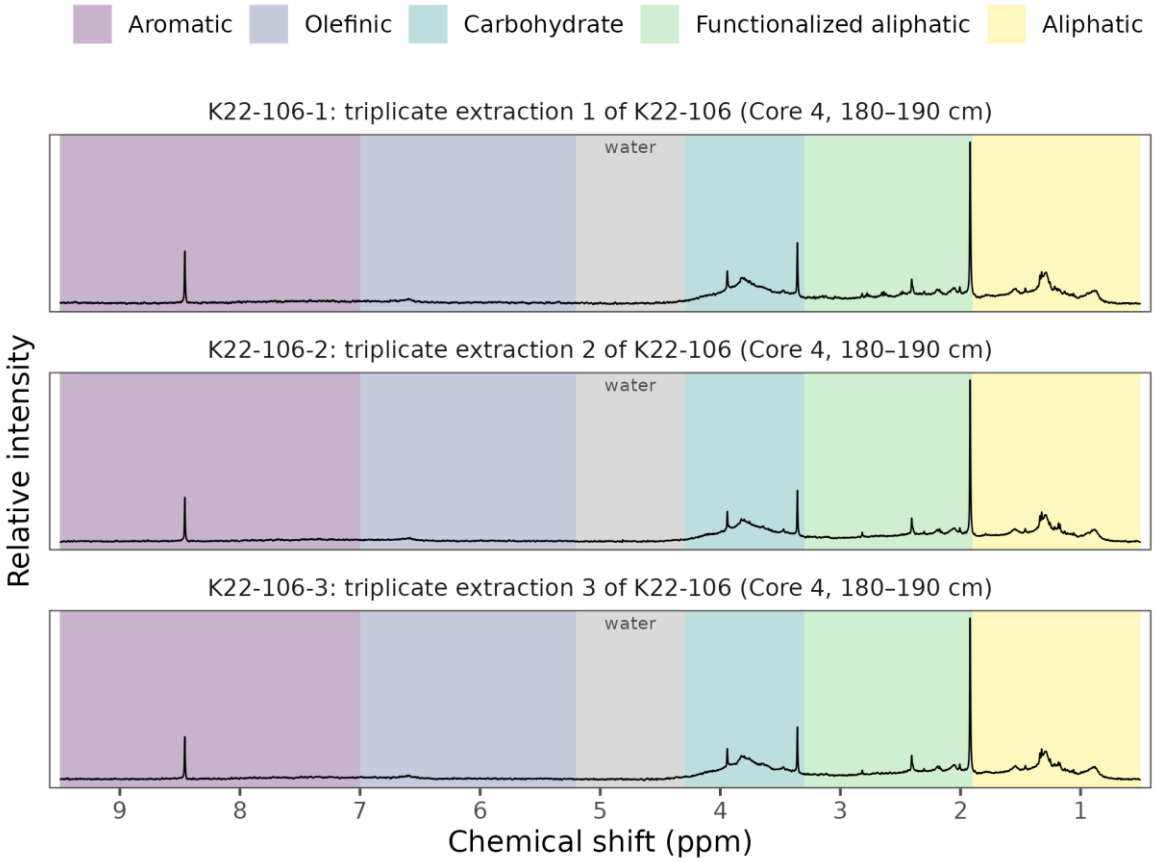


Figure S1. ^{1}H NMR spectra of triplicate extractions (K22-106-1 to K22-106-3) of sample K22-106 (Core 4, 180–190 cm), shown over the full chemical-shift range including the water region (4.3–5.2 ppm, gray), to illustrate reproducibility and water suppression. Each spectrum is scaled to its integral over the five regions; shading marks the integration regions, colored as in Fig. 4. Sharp singlets at 1.92, 3.36 and 8.45 ppm are attributable to acetate, methanol and formate (see main text, Sect. 2.3).

Figure S2

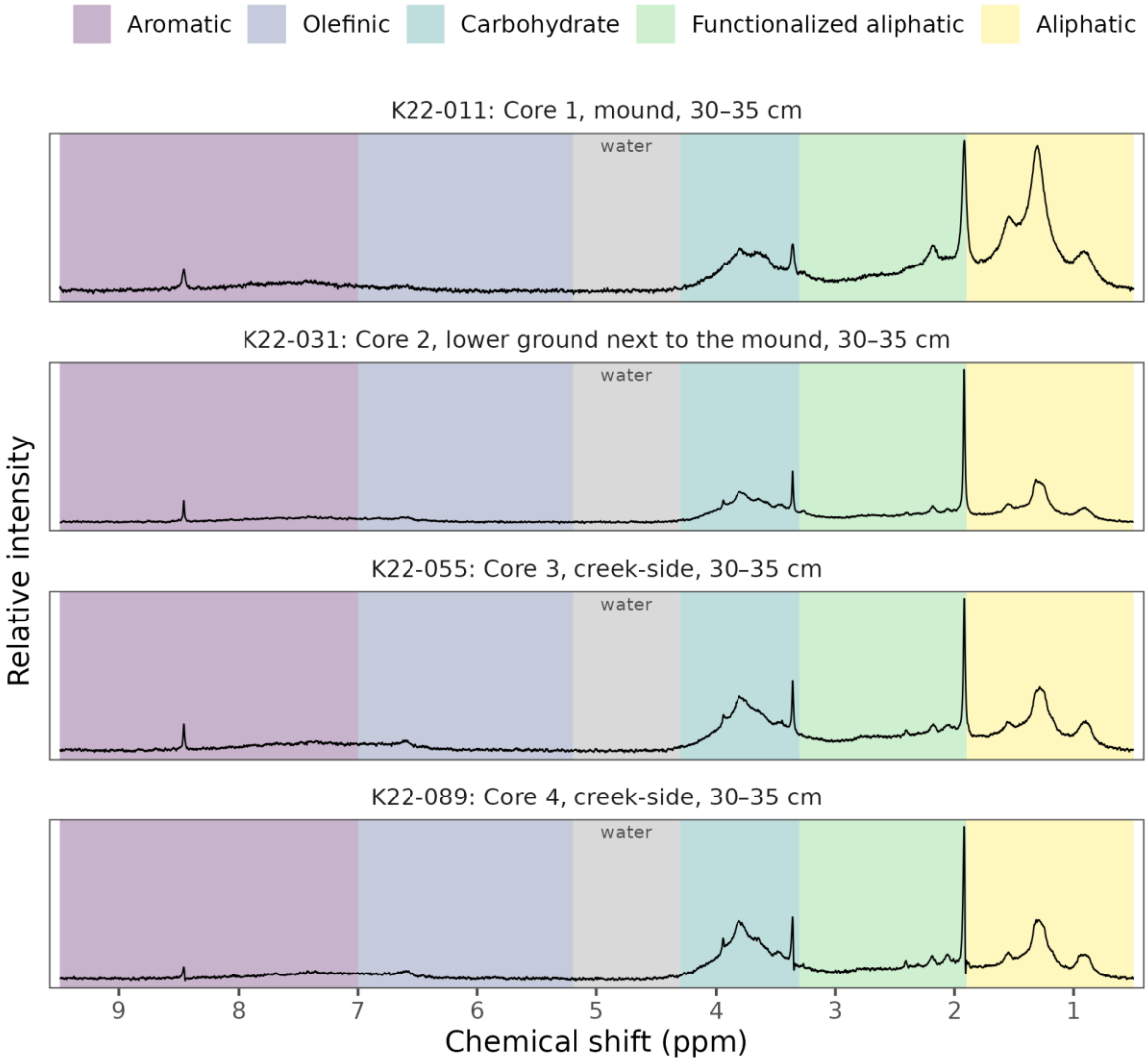


Figure S2. Representative ^{1}H NMR spectra of alkali-extractable OM at 30–35 cm in the four cores, shown over the full chemical-shift range including the water region (4.3–5.2 ppm, gray). This depth was sampled in all cores and had the highest minimum signal-to-noise ratio among them (S/N > 1000; CH_2 peak height at 1.20–1.45 ppm relative to baseline noise at 9.6–10.5 ppm). Each spectrum is scaled to its integral over the five regions; shading as in Fig. S1. The Core 1 spectrum (mound) shows the stronger aliphatic signal typical of that core.

Figure S3

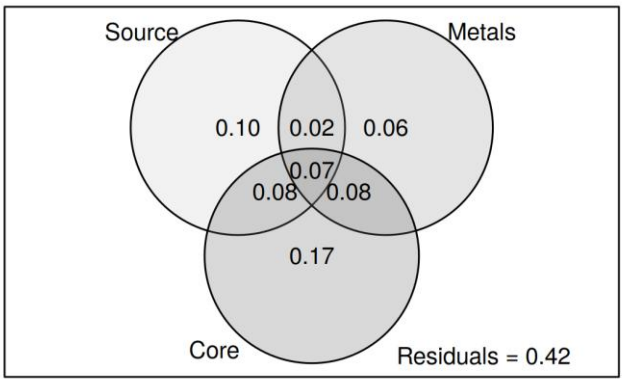


Figure S3. Variation partitioning of the five-region NMR composition (Aitchison distance; adjusted R^2) among source proxies ($\delta^{13}C$, $\delta^{15}N$, C/N), metals (Fe_{pp}, $Fe_{ox} - Fe_{pp}$, Al_{pp}, $Al_{ox} - Al_{pp}$, Ca_{ex}) and core. Values below zero are not shown.

References

Japanese Humic Substances Society: Handbook of Humic Substances Analysis, Sankeisha, Nagoya, 2007 (in Japanese). [check title/publisher]

Martín-Fernández, J. A., Hron, K., Templ, M., Filzmoser, P., and Palarea-Albaladejo, J.: Bayesian-multiplicative treatment of count zeros in compositional data sets, Stat. Model., 15, 134–158, https://doi.org/10.1177/1471082X14535524, 2015.

Wagai, R., Kajiura, M., Uchida, M., and Asano, M.: Distinctive roles of two aggregate binding agents in allophanic Andisols: young carbon and poorly-crystalline metal phases with old carbon, Soil Syst., 2, 29, https://doi.org/10.3390/soilsystems2020029, 2018.

Wagai, R., Kajiura, M., and Asano, M.: Iron and aluminum association with microbially processed organic matter via meso-density aggregate formation across soils: organo-metallic glue hypothesis, SOIL, 6, 597–627, https://doi.org/10.5194/soil-6-597-2020, 2020.